

## CERTAIN ASPECTS OF FAN MODEL STAGE DESIGNING FOR ADVANCED TURBOFANS

S.V. Pankov, V.I. Mileschin, I.K. Orekhov, V.A. Fateev  
Central Institute of Aviation Motors (CIAM), Moscow, Russia

**Keywords:** *test facility, fan, composite materials, performances*

### Abstract

*This work presents numerical and experimental investigations of large-scale fan model stages for low-noise high-performance fan prototypes designed for advanced civil aircraft geared and non-geared turbofans with low and ultra-low rotor tip speeds, high specific capacities, and high by-pass ratios. The stages are intended for tests in the anechoic chamber of the CIAM C-3A unique special acoustic test facility with the aim of verification new methods for optimal designing similar fans to achieve maximum performance.*

### Nomenclature

$D$	–	tip diameter, m
$\bar{d}$	–	relative hub diameter
$F$	–	Flat area, $\pi D^2 \cdot (1 - \bar{d}^2)$ , m <sup>2</sup>
$G$	–	air flow, kg/s
$M$	–	by-pass ratio
$P^*$	–	total pressure, Pa, KPa
$T^*$	–	total temperature, K
$\pi^*$	–	total pressure ratio
$\eta^*_{ad.}$	–	adiabatic efficiency
$\sigma$	–	pressure recovery ratio
$SM$	–	stall margin
$N$	–	rotational speed, r.p.m.
$\bar{n}$	–	$n$ taken relative to a $ADP$
$U$	–	tip speed, m/s
$M$	–	Mach number
$H$	–	flight altitude (height), m, km
$ADP$	–	Aero Design Point (abbr.)
$LPC$	–	Low pressure compressor
$Sh$	–	Strouhal number
$F$	–	vibration frequency
$H$	–	blade height

$b_{0.9}$	–	blade chord at 0.9 height
$w_{0.9}$	–	relative flow rate at the same height

### Indexes

c	–	compressor
igv	–	inlet guide vane
f	–	fan
r	–	rotor
le	–	leading edge
te	–	trailing edge
ogv	–	outlet guide vane
st	–	stage
air	–	air
ad	–	adiabatic
cor.	–	corrected
I	–	inner duct
II	–	outer duct

### mathematical modeling

$(x, r, \varphi)$	–	cylindrical coordinate system
$\bar{q}$	–	conservative variables
$\bar{E}, \bar{F}, \bar{G}$	–	fluxes
$\bar{S}$	–	right-hand side
$P$	–	source term
$k$	–	turbulence kinetic energy
$\omega$	–	specific rate of dissipation

### Subscripts

$v$	–	viscous
$l$	–	laminar
$t$	–	turbulent

### profiling of blade rows

$X(t)$	–	point of the curve
$X_B, X_F$	–	start and end points
$D_B, D_F$	–	tangent vectors
$L$	–	curvature of a line
$T$	–	interval length
$t$	–	parameter
$\tau$	–	normalized parameter

## 1 Introduction

With the aim of refinement the engineering solutions and technologies to ensure designing of new and derivative versions of turbofans for civil haul aircraft with account of competitiveness demands on the world market, general requirements for various families of turbofans are specified and defined more accurately [1, 2]. The engine performance map and other main characteristics for advanced short- and medium-range narrow-body aircraft, as well as long-range wide-body passenger and transport civil aircraft are defined. General requirements for their components and units are laid down. For the purpose of fans improvement, a decision is taken to continue the research and technological groundwork for optimal designing and mathematical modeling of processes, as well as experimental investigations of their aeromechanical and acoustic characteristics at SRC CIAM special test facilities (Russian Federation's State Research Center of the "Central Institute of Aviation Motors named aft. P.I. Baranov") [3].

It is well known that at present, fans with narrow shrouded blades are replaced by high-performance low-noise fans with wide-chord blades. Today, it is especially vital to find means and methods for an additional decrease of noise emission, an improvement of efficiency and stall margins, and a decrease in weight in combination with required service life and high reliability. Achieving these goals is potentially possible by decreasing tip speeds of blades and increasing bypass ratios of fans. It is also interrelated with a progress in manufacturing technologies for hollow blades and blades made of polymer composite materials (PCM). Earlier, for 15-20 years, tip speeds of rotor blades for non-geared civil turbofans have been steadily decreasing from  $U_{f\text{cor.}} \sim 450$  m/s to  $U_{f\text{cor.}} \sim 400$  m/s solely for the purpose of noticeable improvements in acoustic characteristics and efficiency.

High specific capacity in combination with high efficiency ( $> 0.91$ ) of new fans resulted in difficulties due to lack of experience in their developments.

Two small-scale straight-flow fan models ( $U_{f\text{cor}} = 367$  m/s) and ( $U_{f\text{cor}} = 400$  m/s),  $D_r = 400$

mm developed by CIAM in 2003-2008, has made it possible to develop approaches to designing the fans for advanced geared and non-geared turbofans. Both models were manufactured as single-staged in the "rotor + guide vanes" configuration, and rotors of these stages were manufactured as "blisks".

The following clear advantages of experimental studies of small-scale models were taken into consideration: manufacturing time was reduced by 2-3 times with almost 100-fold decrease in cost when the scaling factor was 1: (3 ÷ 5). Therefore, it was easy to manufacture and test a set of single-type units.

The results of tests of these stages at the CIAM UK-3 test facility showed that they provided all key parameters required by the technical design specifications. The first stage in the design mode  $U_{f\text{cor}} = 367$  m/s provided the following values of these parameters:  $G_{f\text{cor}}/F = 200$  kg/s/m<sup>2</sup>,  $\pi_f^* = 1.40$ ,  $\eta_{\text{ad.f}}^* = 0.91$  and the second stage in the design mode  $U_{f\text{cor}} = 415$  m/s provided  $G_{f\text{cor}}/F = 198$  kg/s/m<sup>2</sup>,  $\pi_f^* = 1.60$ ,  $\eta_{\text{ad.f}}^* = 0.91$ .

Using this experience, two large-scale ( $D_f = 700$  mm) model stages for non-geared turbofans with three and four booster stages ( $U_{f\text{cor}} = 405$  m/s) with titanium blades were manufactured for tests in the anechoic chamber of the SRC CIAM C3-A acoustic test facility. Based on test results, a decision was taken to manufacture a full-scale fan for an advanced turbojet engine with the use of a scaled rotor of one of these models.

The tests were carried out at the SRC CIAM C-3A test facility designed for aeromechanical and acoustic testing of counter-rotating or single-row fan models. The test facility, various fan models, as well as results of aerodynamic and acoustic tests were presented earlier, for example, in [3-4].

## 2 Mathematical Aerodynamic Modelling

The fans were designed and computed using methods and algorithms implemented in programs developed by CIAM. For more than 20 years, these methods have been using in calculations of viscous flows of heat-conducting

compressible gas in multi-stage axial and centrifugal compressors and bypass fans.

The mathematical model is based on the numerical solution of the Reynolds-averaged Navier-Stokes equations by the Godunov's scheme (an implicit version with high order accuracy in spatial coordinates) and interfaces between rows of stator vanes and rotor blades of the «mixing plane» type.

Unsteady interactions with changes in the relative position of rotor blades and stator vanes are not taken into account.

### 2.1 Equations of Motion

The equations of motion for viscous heat-conducting compressible gas written in the dimensionless form in relative motion in the cylindrical coordinate system  $(x, r, \varphi)$  rotating around the compressor axis with  $\omega$  angular velocity have a standard form:

$$\partial_t \bar{q} + \partial_x (\bar{E} - \bar{E}_v) + \frac{1}{r} \partial_r r (\bar{F} - \bar{F}_v) + \frac{1}{r} \partial_\varphi (\bar{G} - \bar{G}_v) = \bar{S} - \bar{S}_v,$$

### 2.2 Difference Scheme

Time derivatives in centers of cells are replaced by finite differences. The linearized system of equations is solved iteratively by the method of successive approximations. Flows through the faces are calculated using the solution of the Riemann's problem of breakdown of an arbitrary discontinuity [5]. Parameters on the sides of any face and the derivatives in the centers of cells are calculated in such a way not to disrupt monotonicity by sudden changes in parameters; the order of approximation of the equations in the spatial coordinates should not be lower than the second order. Monotone conservative (shock capture) high order accuracy scheme with TVD limiter [6] is used to solve the system of equations.

### 2.3 Boundary Conditions

Distributions of total pressure and total temperature along the radius in absolute motion as well as the angle between the velocity vector in absolute motion and the meridian plane and the angle between the meridian velocity

component and the compressor axis are specified as the boundary condition at the inlet. The Riemann left invariant is transposed from the computational domain to the inlet boundary along the characteristic. The static pressure is specified at the outlet boundary, and its distribution along the height is derived from the equation of approximate radial equilibrium. The attachment condition is specified on solid walls and the periodicity condition - at the periodic boundaries.

In much the same way as two independent throttle valves in the core and bypass ducts are used in experimental studies of fans for turbojets, setting different values of static pressure at the outlets of these ducts exerts an effect on values of bypass ratio,  $m$ , and other parameters.

### 2.4 Turbulence Simulation

The two-parameter differential turbulence model («k- $\omega$ ») [7,8] with a standard set of coefficients is used in our calculations.

$$\partial_t \rho k + \text{div}(\rho k \bar{w}) = \text{div}((\mu_l + \frac{\mu_t}{\sigma_k}) \nabla k) + P_k - C_\mu \rho k \omega$$

$$\partial_t \rho \omega + \text{div}(\rho k \bar{w}) = \text{div}((\mu_l + \frac{\mu_t}{\sigma_\omega}) \nabla \omega) + \frac{\omega}{k} (\alpha P_k - \beta \rho k \omega)$$

$$C_\mu = 0.09, \sigma_k = 2, \sigma_\omega = 2, \alpha = 5/9, \beta = 3/40$$

The Sutherland's law is used in calculations of laminar viscosity dependence on temperature.

### 2.5 Blade Row Profiling

Designing is preceded by the analysis of prototypes. At first, geometric and gas-dynamic parameters are optimized using the most simplified reduced mathematical models, including multiple 1-D calculations of characteristics along the middle radius. A great number of parameters are taken into consideration. 2-D calculations of axisymmetrical steady flows in direct and inverse problem statements are carried out to find pitch-averaged flow angles with subsequent profiling of all blade rows.

It is assumed that capabilities of mathematical models in 1-D and 2-D approximation are almost exhausted, but they can be useful in the foreseeable future. They include

simple phenomenological approaches. Additional parameters and correction factors in the equations are found empirically. Predictability and reliability of calculations can be improved by a step-by-step transition to more complex mathematical models (RANS, URANS, etc.).

The characteristic properties of equations describing two-dimensional steady axisymmetrical flows [9] in the inverse problem statement depend only on the meridian component of the relative velocity, and not on its total value as in the direct problem statement. In this case, the numerical implementation is simply reduced to central differences because the equations to be solved always have an elliptic form if the meridian component of velocity is lower than sound velocity. See also 2D throughflow calculation method [10].

Identification of the blade row profile shape [11] and inverse boundary value problems in aerodynamics [12] are the problems of the cause and effect analysis (recovery the reasons for the consequences). Laws linking causes and effects are set in the direct formulation - these are differential equations and required boundary conditions. For the system of Euler or Navier-Stokes differential equations, the above-mentioned "causes" are specified as an unknown on the right side of the equation, coefficients or boundaries of the computational domain to find the shape of profiles. Such specific characteristics as in distributions of flow parameters at the boundaries are used as "effects". Mathematically inverse relationships are reflected in their incorrectness eliminated by a fair (in some sense) principle (open profiles, etc.) - the same as in the theory of interpolations and splines in terms of possibility to restore a function based on its known values at certain points using the least-square method.

Profiles in the cross-sections of solid metal rotor blades for earlier tested two fans have an unconventional shape to ensure the required static and dynamic strength as well as to decrease viscous and wave losses. This rotor blade profiling procedure is simply explained in Figure 1 a), b), c).

The aerodynamic profile (see Fig.1a) in the rotor blade cross-section is formed by pressure and suction lines, which cover the middle profile

line found by 2-D axisymmetrical flow calculations with corrections considering incidence and deviation angles.

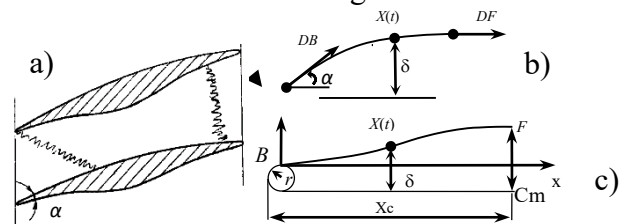


Fig. 1. Rotor blade profiling.

The blade suction side is specified as coinciding with a skeleton surface. The pressure line is formed by two cubic parametric curves with a common point of maximum thickness. The curves can have inflection points and form the specified angles with the profile suction line at leading and trailing edges. The first of these curves -  $X(t)$  is shown in Fig. 1b, 1c. When finding a crosswise blade thickness ( $\delta$ ), the specified thickness of the edge as well as max. thickness of the profile ( $C_m$ ) are taken into account. Directions of tangent lines are specified at the endpoints, i.e. the angle of thickness growth ( $\alpha$ ) is specified at "B" point, and the value of this parameter at "F" point is equal to zero.

A standard presentation of cubic parametric curves is used:

$$X(t) = X_B \cdot (0.5 - \tau)^2(2 + 2\tau) + X_F \cdot (0.5 + \tau)^2(2 - 2\tau) + T \cdot D_B \cdot (0.5 - \tau)^2(0.5 + \tau) + T \cdot D_F \cdot (0.5 + \tau)^2(0.5 - \tau),$$

where  $X$ —point of the curve specified within the interval,  $T$ — distance between extreme points of the interval,  $t$ — parameter,  $T/2 \leq t \leq T/2$ ,  $\tau$  — normalized parameter  $\tau = t \cdot T - 1$ ,  $-0.5 \leq \tau \leq 0.5$ ,  $X_B$ ,  $X_F$  — start and end points,  $D_B$ ,  $D_F$  — tangent vectors at these points.

The line curvature:

$$L = 0.5 \cdot \int_{-H/2}^{H/2} (X_{tt})^2 \cdot dt = 6 \cdot T^{-3} \cdot [X_F - X_B - 0.5 \cdot T \cdot (D_F + D_B)]^2 + 0.5 \cdot T^{-1} \cdot (D_F - D_B)^2$$

— positive quadratic function relatively to  $D_B$  and  $D_F$ . The lines are specified by coordinates of endpoints -  $X_B$ ,  $X_F$  and angles of tangent vectors -  $D_B$ ,  $D_F$ , and their lengths are found from the condition of min.  $L$  value.

This profiling procedure can control the leading edge angle to decrease the intensity of shock waves. The fact that in case of supersonic flow over a wedge with different  $M$ -numbers

(Fig. 2), there is a limiting angle,  $\alpha$ , the supersonic flow can be turned by, i.e. solutions with attached weak oblique shock waves are implemented:

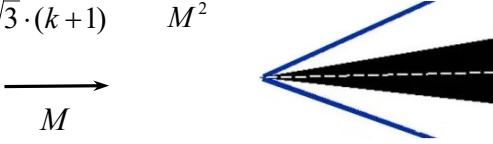
$$\alpha < \frac{4}{3 \cdot \sqrt{3} \cdot (k+1)} \cdot \frac{(M^2 - 1)^{3/2}}{M^2}$$


Fig. 2. Supersonic flow over the wedge

The final shape of profiles in cross-sections of rotor blades is found by combination of available traditional and non-traditional profiling methods.

### 3 Experimental Models

Based on results of first tests of earlier developed large-scale stages ( $D_f = 700$  mm) for non-g geared bypass fans with three and four booster stages, it is found that the declared values of key parameters are achieved.

The measured local flow parameters are close to their calculated values when comparing the distributions along the bypass duct height as well as the integral values in calculations of fan model performances [3,4].

The design features of these fans were also presented earlier, e.g. in [13].

#### 3.1 Non-Geared Fan Model

A decision was taken that one of the earlier studied non-g geared fan models with solid metal rotor blades and four booster stages should be modified. A new non-g geared fan model had substantially different design parameters; configurations of bypass and core ducts were redesigned. The tip speed of rotor blades was reduced by 30 m/s ( $U_{f \text{ cor.}} \sim 370$  m/s), bypass ratio was increased ( $m=11$ ), the rotor's exit hub diameter  $\bar{d}_{te}$  was noticeably reduced, and the rotor blades were to be made of polymer composite materials (PCM).

Preliminary design results were also presented earlier. 3D-RANS calculations of performances showed that the non-g geared fan model could provide high specific capacity and total pressure ratio in bypass and core ducts. The

values of parameters to be provided by the fan in basic operating modes according the technical design specification were slightly corrected, and then the aerodynamic and geometric parameters could be optimized and finally defined.

As to the choice of optimal rotational speeds, it is believed that for any given value of  $\pi_f^*$  we can choose an optimal value of  $U_{f \text{ cor}}$  at which max. value of adiabatic efficiency,  $\eta_{ad, f}^*$ , can be achieved with acceptable stall margins. However, to provide the required thrust owing to high total pressure ratio,  $\pi_f^*$ , optimal rotational speeds of blades,  $U_f$ , can be unacceptably high if blades are made of PCM. In this case, the required value of  $\pi_f^*$  can be achieved by an increase in the loading factor:

$\bar{H}_t = CP \cdot \Delta T^* / U_f^2 \sim U_f^2$ . In other words, the flow turning in interblade channels should be considerably increased, if we assume that  $H_t = CP \cdot \Delta T^*$  changes in accordance with the linear law with changes in the flow angle and in accordance with the quadratic law with changes in rotational speeds of blades.

For example, an experimental model of a highly-loaded fan for a civil aircraft turbofan is presented in [14]. The rotor is manufactured as blisk that results in a decrease in the hub diameter at the inlet with a negligible increase in air flow. However, a decrease in tip speed,  $U_f$ , by 5.4%, calls for an increase in  $\bar{H}_t$  by 17% to keep the same dimensions and thrust.

A decrease in rotor tip speeds and  $\pi_f^*$  leads to a decrease in jet nozzle velocity and a higher flight efficiency, but to ensure the required thrust of the turbofan, air flow in the fan should be higher. High flow velocities at the fan inlet ( $M > 0.7$ ), leads to a high intensity of shock waves and large size of supersonic flow areas. This fact leads to limiting the value of specific capacity,  $G_{a \text{ cor}} / F - \text{max. } 200 \text{ kg}/(\text{s} \cdot \text{m}^2) \text{ or } 220 \text{ kg}/(\text{s} \cdot \text{m}^2)$ , depending on whether the total area, "F", calculated from the outer diameter,  $D_f$  or only the annular duct area with  $\bar{d}_{te} \sim 0.3$  relative hub diameter is taken into consideration. Limiting the value of specific capacity makes it necessary to increase fan dimensions and, consequently, its bypass ratio up to  $m = 10 \div 15$  or higher, but in this case it is necessary to take into account, e.g., an increase in nacelle drag.

The geared fans have advantages in terms of an additional decrease in tip speeds down to  $U_{cor.} < 350$  m/s and even lower  $U_{cor.} = 300$  m/s. In this case, values of  $\eta_{ad,max}^*$  for the compression process will be higher.

### 3.2 Geared fan

At present, an experimental small-scale model stage for a geared fan (1/4.86 scaled model,  $D_f = 700$  mm) is under manufacturing. The stage was modified; implemented adjusting to the test facility and its design documentation was drawn up. In the near future, it will be tested. In conditions of the test facility, it is not proposed to simulate a transition duct and a high-speed LPC installed in the core duct of a full-scale fan.

The calculated values of parameters were presented earlier in [4]. At the design point corresponding to maximum endurance cruise flight at  $M=0.85$ ,  $H=11$ km,  $\bar{n}=1.00$ ,  $U_{f cor.}=313.4$  m/s, the fan model at the test facility should provide the following performance:  $G_{f cor.}/F=198.4$  kg/(s·m<sup>2</sup>),  $\pi_f^* = 1.379$ , and  $\eta_{ad.f}^* > 0.92$ . At the end of climbing ( $\bar{n}=1.04$ ,  $U_{f cor.} = 326.3$  m/s), specific capacity is equal to  $G_{f cor.}/F = 202$  kg/(s·m<sup>2</sup>).

The general view of the fan model installed at the test facility is shown in Fig. 3. Rotor blades made of PCM have ultra-low rotational speeds. Two-row guide vane in the core duct and guide vane in the bypass duct should provide zero value of residual flow swirl at their outlets.

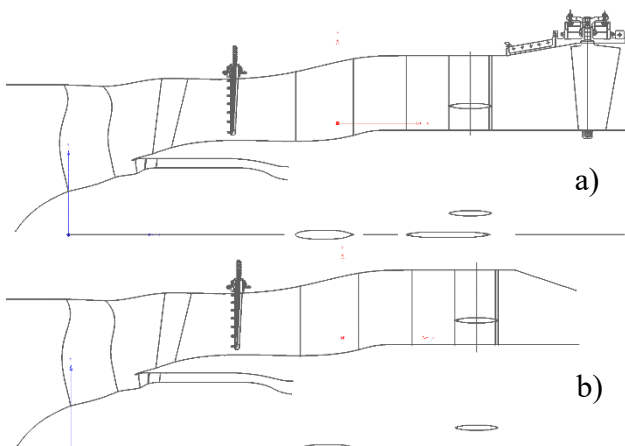


Fig. 3. Geared fan model installed at the test facility. General view.

The experimental performances of the fan can be found in tests with a specially designed vaned diffuser installed at the bypass duct outlet (see Fig. 3a). Acoustic characteristics are measured by a system of replaceable nozzles with different exit areas to provide the required pressure ratio of the fan in "takeoff", "climbing", "descending", "approaching" sideline modes, that is important in view of acoustics certification (see Fig. 3 b).

To ensure experimental investigations, core and bypass duct performances are calculated in basic operating, acoustic, and transient modes at  $\bar{n}_{cor.} = 0.325, 0.480, 0.650, 0.786, 0.906, 0.913, 1.00, 1.041$ . The findings are shown in Fig. 4 and Fig. 5.

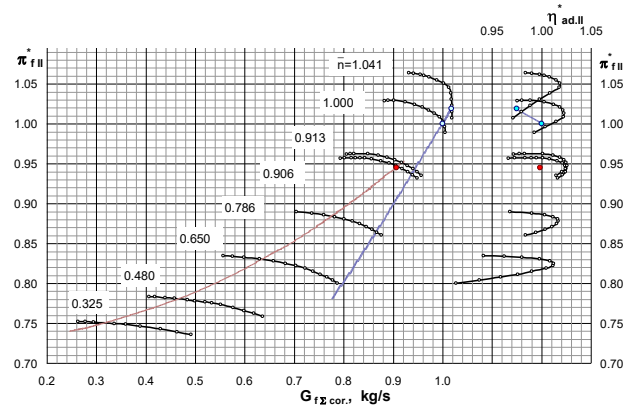


Fig. 4. Calculations of geared fan bypass duct characteristics

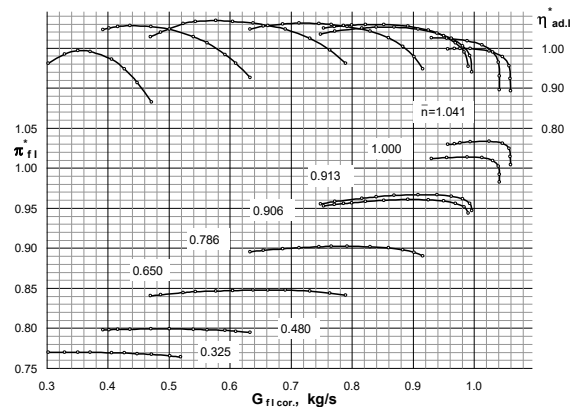


Fig. 5. Calculations of geared fan core duct characteristics

All parameters in Fig. 4, 5 and 6 are shown as ratios to their values at the design point ("Cruise ADP",  $\bar{n} = 1.00$ ).

When calculating the bypass duct performances (see Fig. 4), air flow in the core

duct is specified. When calculating the core duct characteristics, static pressure at the core duct outlet is taken constant along any line in Fig. 5.

The calculated data show that the required values of parameters in the bypass duct can be achieved even with a certain margin in terms of efficiency.

Calculations of the lines of joint operation of the fan and replaceable nozzles having different exit areas are completed. All components in the bypass duct, struts and supports of the test facility are taken into account - up to the nozzle exit area (see Fig. 3b).

The cross-section areas providing required pressure ratios of the fan in basic operating and acoustic modes are calculated. Dimensions of four nozzles are calculated: open, nominal, half-closed and closed. Numerical values in Fig. 6 are the outer radiuses at the nozzle exit in millimeters.

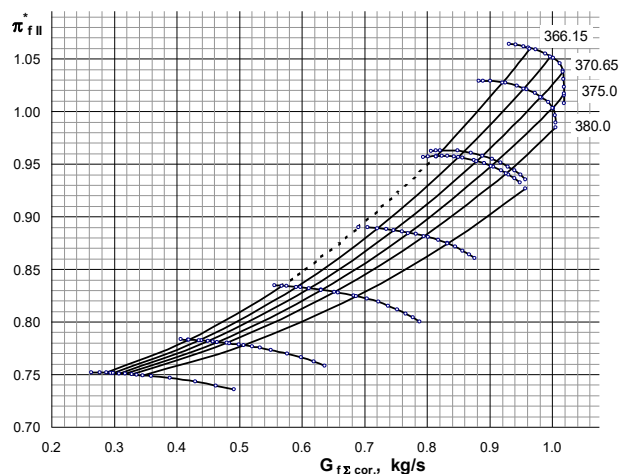


Fig. 6. Calculations of lines of concurrent operation of the fan and replaceable nozzles with different nozzle exit areas

Fig. 7 - Fig. 9 show Mach number distributions in rotor blade and stator vane channels for the most challenging mode - "end of climb":  $\bar{n} = 1.04$ ,  $U_{f\text{ cor.}} = 326.3$  m/s,  $\pi_f^* = 1.405$ .

Max. flow velocity reaches  $M_{max.} = 1.4$  on suction sides in rotor blade tip sections (Fig.7).

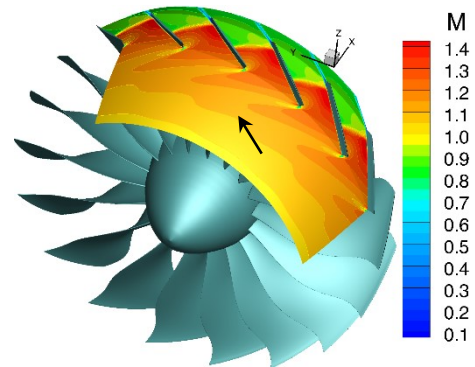


Fig. 7. Mach number distribution in the inter-blades channels of fan rotor.

On suction sides of the first-row stator vanes in the core duct,  $M_{max.} = 1.15$ . Axis of the second row is not radial; deflection of vanes along the height is clearly visible; flow velocity in this row is lower than sound velocity (Fig. 8).

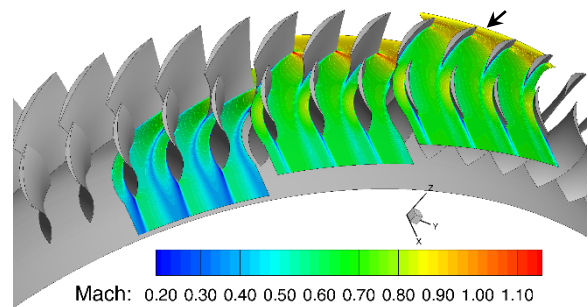


Fig. 8. Mach number distribution in the fan core duct in inter-blades channels of two-row guide vanes.

Maximum velocity hardly exceeds the sound velocity ( $M_{max.} = 1.05$ , see Fig. 9) on the suction sides of guide vanes in the bypass duct near the intermediate casing.

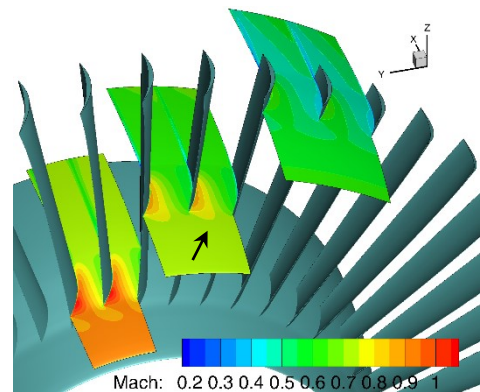


Fig. 9. Mach number distribution in the fan bypass duct inter-blades channels of guide vanes.

#### 4 Strength calculations of fans

For a breakthrough in manufacturing technologies, shroudless wide-chord rotor blades for new fan models should be made of polymer composite materials (PCM).

They are manufactured with a variable sweep along the blade height, and their sailary is above 1. For example, sailary of rotor blades in geared fan is equal to  $b_{tip}/b_{hub} = 1.467$ , and their aspect ratio is  $h_{le}/b_{mid} = 1.905$ .

The intricate shape of blade profiles in cross sections is chosen to provide the required static and dynamic strength, as well as to reduce viscous and wave losses. All features of PCM blade manufacturing are taken into account; thickness of blade edges and max. thickness in root sections are increased.

Initially, two sets of blades made of titanium alloy and a polymer composite material are to be manufactured and tested. The titanium solid blade is composed of an airfoil, a foot, and a shroud-type root. The PCM blade is composed of an airfoil and a foot with an aluminum shroud. Metal and composite blades should have the same shape in hot state at the design point (cruise flight)  $n=1.00$  in conditions of max. endurance flight at  $M=0.85$ ,  $H=11\text{km}$ . Static strength of blades is provided in the most challenging ground test conditions -  $n=1.04$  owing to a correct choice of the meridional projection shape and distributions of max. thickness of blade profiles along the height with account of technological limitations associated with thickness of one layer of the material. To ensure high strength of reinforcing fibers, they should be laid with max. possible radius. Small radius results in inadmissibly low strength.

The fan model is an exact scaled-down copy of a full-scale fan but 5-times reduced that leads to a decrease in the fiber bend radius by the same times. Therefore, static strength of model blades is lower than full-scale blades, but this is admissible because of their required short life.

Resonant vibrations of blades for first waveforms excited by first six harmonics of circumferential flow non-uniformity in max. design conditions are tuned out. Analysis of dynamic characteristics of the blades was

presented earlier in the form of the Campbell resonance diagram [4].

Well-known types of flutter are tuned out by the choice of blade aspect ratios, distributions of maximum thickness along the blade height and circumferential positions of cross-sections with limitations on the static strength. The absence of flutter is provided by the choice of Strouhal numbers  $Sh=2\pi f b_{0.9}/w_{0.9}$  ( $f$  – vibration frequency,  $b_{0.9}$  – blade chord at  $\bar{h}=0.9$  height,  $w_{0.9}$  – relative flow rate at the blade inlet at the same height), which should be higher than its critical values separating the reliably flutterless area. Critical values of Strouhal numbers are found statistically by processing reported flutter events in rotors of aircraft GTE's axial fans and compressors. The absence of bending-torsional flutter is provided by an admissible relative difference between second bending and first torsional frequencies.

Because of decreased relative flow velocity, at low rotational speeds of rotor blades even with small thickness it is easier to provide required margins of torsional and bending flutters as well as reserves for 1-st mode vibrations with 1-st harmonic excitation frequency and 2-nd mode vibrations with 3-rd harmonic excitation frequency.

Static strength of guide vanes in the core and bypass ducts is provided.

#### 5 Conclusions

The authors consistently adhere to the present-day well-elaborated paradigm of designing and experimental studies of model stages for prototypes of high-performance low-noise conventional geared and direct-driven fans, in order to assess and reduce possible risks in developments of new and upgraded civil aircraft turbofans to give them an edge over their competitors.

At present, it is important to develop a ground-breaking manufacturing technology for lightweight and high-strength blades made of polymer composite materials. Therefore, rotor blades for new fan models will be made of PCM.

The most challenging is achievement of high parameters in the fan core duct in view of a

reduced rotor's exit hub diameter and low tip speeds of rotor blades.

In the near future, long-expected experimental studies of aerodynamics and noise of the geared fan model currently under manufacturing with ultra-low rotational speeds of rotor blades will be of great interest.

## References

- [1] Parker, R., Babkin, V. Challenges of Advanced Propulsion Systems Development for Air Transport Flying by 2035-2050. *ICAS2014*, ICAS-2014-0.2
- [2] Lanshin, A.I., Mirzoyan, A.A, Polev, A.S. Development of Technology Advance for Future Propulsion Systems of Haul Aircraft of Development Gas-turbine Engines for Subsonic Civil Aircraft. *ICAS2016*, ICAS2016\_0542.
- [3] Pankov, S.V., Mileschin, V.I., Korzhnev, V.N Numerical and Experimental Investigations Bypass-flow Fans for an Advanced Civil Aircraft Engine. *ICAS2014*, ICAS2014\_0104.
- [4] Pankov, S.V., Mileschin, V.I., Orechov, I.K. Fateev V.A Development of the Fan Stage with Ultra-Low Rotational Speed *ICAS2016* ICAS2016\_0542.
- [5] Godunov S.K., (1959) "A Difference Scheme for Numerical Solution of Discontinuous Solution of Hydrodynamic Equations", *Math. Sbornic*, 47, 271–306, translated US Joint Publ. Res. Service, JPRS 7226, 1969. Cornell Aeronautical Lab. Transl.
- [6] Anderson, W.K., Thomas, J.L. and Van Leer, B., "A Comparison of Finite Volume Flux Vector Splittings for the Euler Equations", *AIAA Paper* No. 85-0122, January 1985
- [7] Wilcox, D.C. Multiscale Model for Turbulent Flows. In *AIAA J.* 26,1311-1320., 1988.
- [8] Stephen B. Pope. *Turbulent Flows*. Cambridge university press, 2000.
- [9] Katsanis, T., McNally, W.D. Revised Fortran Program for Calculating Velocities and Streamlines on a Blade-to-Blade Stream Surface of a Turbomachine. NASA TMX 1764, 1969
- [10] Mingzhi Tang, Donghai Jin, Xingmin Gui. Modeling and Analysis of the Inlet Circumferential Fluctuations in Subsonic Rotors. *GT2017-63929*, ASME-2017, June 26-30, *Charlotte, NC, USA*.
- [11].H.-J. Lichtfuss. Customized Profiles - the Beginning of an era., A Short History of Blade-Design. *Proceedings of ASME Turbo Expo, GT2004-53742*, June 14-17, 2004, Vienna, Austria.
- [12] Garabedian P.R., Korn D.G. Numerical design of transonic airfoils. In: Numerical solution of partial Differential Equations. II. New York; Press. 1971. – P.253-271.

- [13] Lisa Brilliant, Stanley Balamucki, George Burger, Yuan Dong, and Charlie Lejambre. Application of Multistage CFD Analysis to Low Pressure Compressor Design. *GT2004-54263*, ASME-2004, June 14-17, *Vienna, Austria*.
- [14] Jens Nipkau, Bronwyn Power Matthew Jordan. Aeromechanical Design and test of Modern Highly Loaded Fan. *GT2017-64630*, ASME-2017, June 26-30, *Charlotte, NC, USA*.

## 8 Contact Author e-mail addresses:

mail to: [pankov@ciam.ru](mailto:pankov@ciam.ru), [mileschin@ciam.ru](mailto:mileschin@ciam.ru), [ig.orekhov@mail.ru](mailto:ig.orekhov@mail.ru), [fateev@ciam.ru](mailto:fateev@ciam.ru),

## Copyright Statement

The authors confirm that they, and/or their company or organization, hold copyright on all of the original material included in this paper. The authors also confirm that they have obtained permission, from the copyright holder of any third party material included in this paper, to publish it as part of their paper. The authors confirm that they give permission, or have obtained permission from the copyright holder of this paper, for the publication and distribution of this paper as part of the ICAS proceedings or as individual off-prints from the proceedings.